Calculation of ozone line shifting induced by N2 and O2 pressure

Nina Nikolaevna Lavrentieva, Anna Sergeevna Osipova, Jeanna Buldyreva

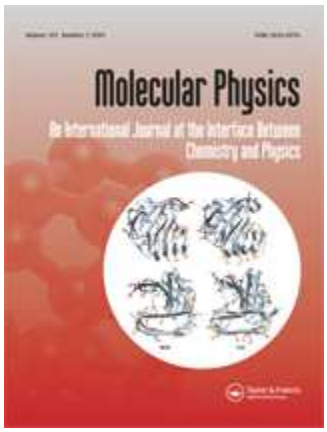

Calculation of ozone line shifting induced by N2 and O2 pressure

Journal:	*Molecular Physics*
Manuscript ID:	TMPH-2009-0156.R1
Manuscript Type:	Full Paper
Date Submitted by the Author:	01-Jun-2009
Complete List of Authors:	Lavrentieva, Nina; Institute of Atmospheric Optics Osipova, Anna; Tomsk State University Buldyreva, Jeanna; Université de Franche Comté, UTINAM
Keywords:	ozone, line shift, semiempirical calculation, polarizability in excited vibrational state, temperature exponent

Calculations of ozone line shifting induced by N_2 and O_2 pressure

N. Lavrentieva [a], A. Osipova [b] and J. Buldyreva [c*]

[a] Institute of Atmospheric Optics, 1 ave Akademicheskii, 634055 Tomsk, Russia

[b] Tomsk State University, 36 ave Lenina, 634050, Tomsk, Russia

[c] Institut UTINAM, UMR CNRS 6213, Université de Franche-Comté, 16 route de Gray, 25030 Besançon cedex, France

[*] Corresponding author ; Phone: +33 (0)3 81 66 63 60; FAX: +33 (0)3 81 66 64 75; Electronic address : jeanna.buldyreva@univ-fcomte.fr

Abstract

Ozone line shifts by nitrogen and oxygen pressure are computed for the $\nu_1+\nu_3$, $2\nu_1$ and $2\nu_3$ bands of the 5μm spectral region by a semiempirical approach. The calculated values agree with measurements better than 0.001 $cm^{-1}atm^{-1}$ for 98% of O_3-N_2 lines and 87% of O_3-O_2 lines. In contrast with the water molecule case, the polarization components of the interaction potential are shown to contribute to the line shift more efficiently than the electrostatic interactions. As intermediate results, the mean dipole polarizability and the components of the polarizability tensor for the vibrational states (101), (200), and (002) of ozone molecule are determined by least-squares fitting of theoretical shifts to some experimental values. The temperature exponents for the $\nu_1+\nu_3$ band lines are also estimated.

Keywords: ozone, line shift, semiempirical calculation, polarizability in excited vibrational state, temperature exponent

I. Introduction

Among the minor constituents of the Earth's atmosphere ozone receives a particular attention of scientists due to its double role of protector and pollutant: whereas the stratospheric ozone layer protects the humans, animals and vegetation from the harmful ultraviolet radiation of the Sun, the excessive concentration of ozone in the troposphere is qualified as pollution because of its toxic effects for respiration. Precise measurements of vertical ozone concentration profiles are therefore of crucial importance for health protection services and scientific community interested in comprehension and global modelling of the terrestrial atmosphere.

The probing of atmospheric species is principally realized by non intrusive spectroscopic techniques in the infrared, microwave and millimeter domains. For ozone, the spectral regions of 5 μm and 10 μm are of particular interest since they correspond simultaneously to its most intense absorption bands and to "atmospheric windows" free of water vapour absorption. Reliable inversion of the recorded spectra requires a precise knowledge of ozone spectral line shape parameters (including its main isotopic species) in a wide temperature range and in different vibrational bands.

While the ozone line broadening has been quite intensively studied both experimentally and theoretically, its line shifting data remain quite sparse. Only some measurements were made by Smith et al. [1-4], Barbe et al. [5-6] and Sokabe et al. [7] and only QFT (Quantum Fourier Transform) and ATC (Anderson-Tsao-Curnutte) calculations were realized by Gamache and co-workers [8-9] for N_2, O_2 and air-broadening. Recently, the complex-valued version of the Robert-Bonamy formalism was employed by Drouin et al. [10] to estimate line shifts induced by the same perturbers in the rotational band of O_3; no experimental data were reported however for comparison because of their too small values. From the theoretical point of view the line shifting mechanism has a more

complicated character than the line broadening, and many factors negligible for the width become important for the shift (strong dependencies on vibrational quantum numbers, type of perturbing molecules, isotopic species). Since the pressure shift is more sensitive to the intermolecular interaction details than the line broadening, it represents a very promising tool for molecular collision studies. An exhaustive analysis of available experimental data and calculation of line shifts induced in particular by nitrogen and oxygen are therefore of great importance for better understanding of the shifting mechanism and improvement of our knowledge of the ozone spectroscopic properties.

In this paper we present a first systematic calculation of O_3-N_2(O_2) vibrotational line shifting coefficients and of their temperature dependence for three vibrational bands of the 5μm region ($\nu_1+\nu_3$, $2\nu_1$, $2\nu_3$) by a semiempirical method developed previously [11] and successfully applied to the case of O_3-N_2(O_2) line broadening [12]. In the frame of this approach the impact theory is modified by introducing additional semiempirical parameters determined by fitting to experimental data. They are used further to calculate the line shifts which have been not measured. This method gives the possibility to calculate separately the contributions to the line shape parameters from different types of intermolecular interactions and from different scattering channels, which enables an analysis of vibration-rotational dependence of the shifting coefficients for various kinds of perturbers.

II. Method of calculation

The semiempirical method [11] has been already used for calculation of line shape parameters and their temperature exponents for H_2O-N_2, H_2O-O_2, H_2O-H_2O_2, CO_2-N_2 and CO_2-O_2 molecular systems [13-20]. In Refs [13-19] it has been shown that for polar active molecules the semiempirical approach gives quite accurate parameters values. The results of these calculations are actually included in a freely-available carbon dioxide spectroscopic data bank [21] and in the “ATMOS” Information System [22].

In the framework of this approach the line shift corresponding to the radiative transition from the initial state *i* to the final state *f* depends on the transition probabilities $D^2(ii'|l)$ and $D^2(ff'|l)$ of the different scattering channels connecting the levels *i* and *f* with their neighbouring levels:

$$\delta_{if} = B(i, f) + \sum_{l,i'} D^2\left(ii'\middle| l\right)P_l\left(\omega_{ii'}\right) + \sum_{l,f'} D^2\left(ff'\middle| l\right)P_l\left(\omega_{ff'}\right) + \ldots \quad (1)$$

(the higher order terms are neglected). These transition probabilities represent the squared reduced matrix elements of the relevant molecular operators such as the components of the dipole moment (tensorial order l = 1), the components of the quadrupole tensor (l = 2) or the components of higher multipoles. The expansion coefficients $P_l(\omega)$, called in the literature "interruption" or "efficiency functions", depend on the intermolecular potential, the trajectory, the energy levels and the wave functions of the perturbing molecule. They can be seen as interruption functions for a given scattering channel and can be formally written as a product of the interruption function of the ATC theory $P_l^{ATC}(\omega)$ and of a correction factor $C_l(\omega)$ deduced from fitting to experimental data:

$$P_l(\omega) = C_l(\omega)P_l^{ATC}(\omega). \quad (2)$$

In order to account for the rotational dependence of the interruption function the form of this correction factor is chosen as

$$C_l(\omega) = \frac{c_1}{c_2\sqrt{J}+1} \quad , \quad (3)$$

where the fitting parameters c_1 and c_2 are responsible respectively for the correction of errors induced by the cut-off procedure and the vibrational dependence. These parameters values c_1 = 2.7 and c_2 = 7.0 were taken from our previous work [12] on the $\nu_1+\nu_3$ band line broadening coefficients (fitting to some experimental values from *R*- and *P*-branches with various values of the rotational quantum number *J*) and used here for three considered vibrational bands without any change. This fact confirms the internal consistency of the

semiempirical approach for simultaneous prediction of both line widths and line shifts.

The first term $B(i, f)$ appearing in Eq. (1) accounts for the contribution of the isotropic part of the interaction potential:

$$B(i,f) = \frac{n}{c} B_1 \left[\alpha_2 (\mu_f^2 - \mu_i^2) + \frac{3I\, I_2 (\alpha_f - \alpha_i)}{2(I + I_2)} \right] \sum_p \rho(p) \int_0^\infty v F(v) b_0^{-3}(v, p, i, f) dv \,, \qquad (4)$$

where n is the number density of the perturbing molecules and ρ is the population of their different (rotational) states p, the constant B_1 = -3π/(8ħν), and $\alpha\,(\alpha_2)$, μ, $I\,(I_2)$ are, respectively, the mean polarizability, dipole moment, and ionization potential of the active (perturbing) molecule. The integration on the relative molecular velocity v is made with the Maxwell-Boltzmann distribution function $F(v)$ and b_0 means the interrupting radius. In the excited vibrational states the mean dipole polarizability is not well known whereas through Eq. (4) it is responsible for the (very clearly pronounced) vibrational dependence of the line shifting coefficient. In our calculations we therefore considered it as an additional fitting parameter.

Equation (1) for the line shift can be expressed in terms of the conventional ATC interruption functions $S_1(b)$ and $S_2(b)$ which depend on the impact parameter b and correspond to the contributions from the isotropic and anisotropic parts of the interaction potential, so that

$$S_1(b) = B(i, f), \qquad (5)$$

$$S_2(b) = \sum_{l, i'} D^2 \left(ii' \middle| l \right) P_l(\omega_{ii'}) + \sum_{l, f'} D^2 \left(ff' \middle| l \right) P_l(\omega_{ff'}) \,. \qquad (6)$$

For O_3-$N_2(O_2)$ case the $S_2(b)$ contribution can be written as

$$S_2(b) = S_2^{12e}(b) + S_2^{22e}(b) + S_2^{22p}(b) + S_2^{02p}(b) + S_2^{20p}(b) \,, \qquad (7)$$

where the numerical superscripts denote the multipolarity of the interactions for the active and perturbing molecules and the superscripts e and p denote respectively the electrostatic

and the polarization parts of the interaction potential. Namely, the terms $S_2^{12e}(b)$ and $S_2^{22e}(b)$ come from the dipole-quadrupole and quadrupole-quadrupole interactions whereas the terms $S_2^{22p}(b)$, $S_2^{02p}(b)$ and $S_2^{20p}(b)$ are due to the polarization and dispersion contributions. Their detailed expressions can be found in [23, 24]. According to Eq. (4) the interruption function $S_1(b)$ related to the isotropic potential is determined by $\mu_f^2 - \mu_i^2$ and $\alpha_f - \alpha_i$ differences. The terms $S_2^{22p}(b)$, $S_2^{02p}(b)$ and $S_2^{20p}(b)$ depend on $\alpha_i - \alpha_i^{zz}$, $\alpha_f - \alpha_f^{zz}$, $\alpha_i^{xx} - \alpha_i^{yy}$, and $\alpha_f^{xx} - \alpha_f^{yy}$ values, where $\alpha_{i(f)}^{xx}$, $\alpha_{i(f)}^{yy}$, $\alpha_{i(f)}^{zz}$ are the Cartesian components of the polarizability tensor of the absorbing molecule in the initial (final) states.

In [25] it has been shown that the vibrational dependence of the line shift coefficients of water vapour is explained by the intermolecular potential: the shift is mainly determined by the polarization term $S_1(b)$ and the electrostatic term $S_2^{12e}(b)$. In contrast with the water vapour molecule, the ozone molecule has a three times smaller dipole moment (0.53 D) while a two times greater mean polarizability (2.8 Å^3) in the fundamental vibrational state. Therefore for O_3-$N_2(O_2)$ interactions the second-order polarization contributions $S_2^{22p}(b)$, $S_2^{02p}(b)$ and $S_2^{20p}(b)$ are expected to be significant, and in addition to the electrostatic terms we accounted in our calculations for the interactions like dipole-induced dipole. The polarization contributions to $S_2(b)$ were calculated using the resonance functions Ig_1 and Ig_2 determined earlier in [26].

In the present study we have determined the components of the polarizability tensor of the ozone molecule responsible for induction and dispersive interactions. The components for the ground vibrational state were measured in [27] and calculated in [28], the first derivatives of the polarizability with respect to the normal coordinates were also determined, but not the second derivatives necessary for estimating the polarizability in the excited states. For our purposes, the polarizability in the upper vibrational state α_f and the

α_f^{zz} component of the polarizability tensor were obtained by least-squares fitting to several experimental line shifts induced by nitrogen pressure, for each band separately. Since the *xx*- and *yy*-components have close values, the difference $\alpha_f^{xx} - \alpha_f^{yy}$ was taken equal to its ground vibrational state value. The adjusted parameters α_f and α_f^{zz} were further used to calculate the line shifts due to oxygen pressure. Table 1 gathers molecular and spectroscopic constants for ozone, nitrogen and oxygen used in our calculations.

III. Results and discussion

For the $\nu_1+\nu_3$ band (J = 2–43) calculated O_3-$N_2(O_2)$ line shift coefficients are presented in Table 2 **(lines used for fitting are marked with asterisk)** together with the corresponding experimental values from Ref. [5]. These measurements were obtained with the spectral resolution of 0.002 cm^{-1} and the accuracy of the line shift coefficients estimated at $2.5 \cdot 10^{-4} cm^{-1} atm^{-1}$ (12%) for most lines ($15 \le J \le 30$, $K_a \le 6$) and at $4 \cdot 10^{-4} cm^{-1} atm^{-1}$ for other lines ($J < 15$, $J > 30$, $K_a > 6$). It is clearly seen from this table that the line shifts by collisions with oxygen molecules are greater than those by collisions with nitrogen molecules. This fact is due to an increasing contribution from $S_1(b)$ (which is always negative) with decreasing interrupting radius b_0. By the way, it leads to the corresponding decrease of the broadening coefficients. Comparison of calculated values with experimental data shows a very good agreement between them: the difference $\Delta = \left| \delta^{expt} - \delta^{calc.} \right|$ does not exceed 0.001 cm^{-1} atm^{-1} for 98% of O_3-N_2 lines and 87% of O_3-O_2 lines with the standard deviation of $7.04 \cdot 10^{-5}$ $cm^{-1} atm^{-1}$. The details of statistics are given in Table 3.

The K_a-dependence of the $\nu_1+\nu_3$ band transitions can be seen on Fig. 1 where a specific combination of the quantum numbers (J + 0.1K_a) allows separation of the lines with identical J-values but different K_a-values (the J-interval starts with J=21 for which K_a=7 and K_a=8 are available). As can be seen from this figure, for some high J

values (J = 26, 31, 32) the calculation reproduces correctly the general behaviour of the experimental K_a-dependences (line shift increases and then decreases with K_a increasing). It is not however the case for other values of J because of the semiempirical character of our model: fitting to some arbitrary chosen experimental values allows a global minimisation of deviations from experimental points but not reproducing fine details in K_a-dependences.

To analyze the vibrational dependence of shifting coefficients, in addition to the band $\nu_1+\nu_3$ two other bands $2\nu_1$ and $2\nu_3$ were studied for the case of nitrogen broadening. Our theoretical and experimental [6] values for these **two bands are given in Tables 4-5.** The general comparison of the results for three studied bands shows that the (absolute) line shifts for $2\nu_1$ band are smaller than those of $\nu_1+\nu_3$ and $2\nu_3$ bands. Indeed, because of the strong polarizability of the ozone molecule the shift becomes noticeable already for transitions to low vibrational states and increases even more for higher vibrational frequencies. A strong vibrational effect and a rotational dependence thus should be noted for the ozone line shifting coefficients. **It is difficult to analyse the K_a-dependence for these bands since only in the $2\nu_1$ band and only for two J-values (J = 26, 29) a couple of various K_a values (K_a =0, 1 and K_a =5, 6, respectively) are available. As shows Fig. 2, for these J-values the experimental shifts decrease whereas the calculated shifts increase when passing from K_a =0 (or K_a =5) to K_a =1 (or K_a =6), which can be explained again by the semiempirical character of our approach.**

An additional point of our work consisted in evaluation of the temperature dependence of line shifts. The temperature exponents N were determined using the relation

$$\delta_{if}(T) = \delta_{if}(297)\left(\frac{T}{297}\right)^{-N}, \qquad (8)$$

where $\delta_{if}(297)$ is the shift value at the reference temperature 297 K. This kind of relation is widely used in the literature and in HITRAN database to characterise the temperature

dependence of the line widths, but mainly for historical reasons since it is valid for molecules interacting through a potential $r^{-\eta}$ [29–31] and can lead to negative values of the temperature exponents for certain transitions of H_2O perturbed by nitrogen, oxygen or air [32, 33]; for rotational transitions of O_3 perturbed by air this relation was found to be correct for the temperature range 225-350 K but not for the 150-450 K [10]. For the line shifts this relation works well [18] when the shift behaviour with temperature variation is quite regular (Eq. (8) does not describe a change of sign). It is the case for the shifts considered in the present paper. We note for completeness, that a similar formula for the line shift temperature dependence was proposed by Gamache and Rothman [34] which introduces a temperature-dependent sign but is not zero at intermediate temperatures; for our case their expression is equivalent to Eq. (8).

Line shift calculations were carried out for five temperatures (200, 230, 260, 297 and 330 K), and the corresponding N values were extracted by a least-squares fitting procedure. For all studied lines the standard deviation did not exceed 10^{-6} $cm^{-1}atm^{-1}$. **Figure 3 shows an example of temperature dependence for the shift of the line 25 5 20 ← 26 5 21 from the $\nu_1+\nu_3$ band (upper panel) and the corresponding plot in logarithmic coordinates (lower panel). The practically linear dependence of $\ln\{\delta(T)/\delta(297)\}$ on $\ln(T/297)$ confirms the validity of Eq. (8) for the temperature dependence of line shifts. For the $\nu_1+\nu_3$ band of O_3-N_2 system the temperature exponent values are given in Table 2.** As can be seen from this table, N varies slightly from 0.74 to 1.15 for the lines with J = 9 - 43, with the mean value equal to 0.986. It should be noted that these calculations refer to the lines with $\Delta K_a = 0$ and $\Delta K_c = 1$ (for other transitions the temperature exponent values can be in principle quite different).

A very rough theoretical estimation of the temperature exponent values for Eq. (8) can be made with the formula obtained by Pickett [35]:

$$N = 1 + \frac{3}{2\eta - 2}, \tag{9}$$

which gives N =1.5 for the dipole-quadrupole (η = 4) and N =1.375 for quadrupole-quadrupole (η = 5) interactions. Our results are therefore quite consistent with these estimations.

IV. Conclusions

The comparison of our calculations with experimental values argues that the semiempirical method is quite acceptable for estimating the shifts of ozone vibrotational absorption lines. For this molecule the polarization components of the interaction potential are shown to contribute to the line shift more effectively than the electrostatic dipole-quadrupole interaction (which is very significant for the line broadening). Whereas for the ozone line broadening by nitrogen and oxygen the vibrational effects are very weak, its line shifts demonstrate a strong vibrational dependence. For accurate calculation of ozone line shift coefficients it is therefore necessary to account for this dependence in some components of the ozone polarizability tensor and its polarizability in the excited vibrational states. These components are determined in the present work for (101), (200) and (002) vibrational states by fitting to experimental data. The temperature dependence of the line shifting coefficients is additionally studied. In general, the mechanisms responsible for the ozone line shifting appear to be much more complex than those responsible for the line broadening, which should be permanently kept in mind when calculating its line shape parameters.

The calculated values are intended for use in spectroscopic databases, for example, the "ATMOS" Information System (http://saga.atmos.iao.ru).

Acknowledgements

The authors acknowledge the financial support by the French national program LEFE-CHAT and by the program "Optical Spectroscopy and Frequency Standards" of the Russian Academy of Sciences.

References

1. M.A.H. Smith, C.P. Rinsland, V. M. Devi, D.C. Benner, and K.B. Thakur, J. Opt. Soc. Am. B 5, 585-592 (1988).
2. M.A.H. Smith, C.P. Rinsland, V. Malathy Devi, E.S. Prochaska, J. Mol. Spectrosc. 164, 239-259 (1994); Erratum, J. Mol. Spectrosc. 165, 596 (1994).
3. M.A.H. Smith, V. Malathy Devi, D.C. Benner, C.P. Rinsland, J. Mol. Spectrosc. 182 (1997) 239-259.
4. V. Malathy Devi, D.C. Benner, M.A.H. Smith, C.P. Rinsland, J. Mol. Spectrosc. 182, 221-238 (1997).
5. A. Barbe, S. Bouazza, J.J. Plateaux, Appl. Opt. 30, 2431-2436 (1991).
6. A. Barbe, J.J. Plateaux, S. Bouazza, Proceedings of the Tenth All-Union Symposium on High Resolution Molecular Spectroscopy, SPIE 1811, Washington, USA, 83-102 (1991).
7. N. Sokabe, M. Hammerich, T. Pedersen, A. Olafsson, J. Henningsen, J. Mol. Spectrosc. 152, 420-433 (1992).
8. R.R. Gamache, L.S. Rothman, Appl. Opt. 24, 1651-1656 (1985).
9. R.R. Gamache, R.W. Davies, J. Mol. Spectrosc. 109, 283-299 (1985).
10. B. J. Drouin, J. Fischer, R.R. Gamache, J. Quant. Spectrosc. Radiat. Transfer 83, 63-81 (2004).
11. A. Bykov, N. Lavrentieva, L. Sinitsa, Mol. Phys. 102, 1653-1658 (2004).
12. J. Buldyreva, N. Lavrentieva, Mol. Phys. 2009 (in press).
13. A. Valentin, Ch. Claveau, A. Bykov, N. Lavrentieva, V. Saveliev, L. Sinitsa, J. Mol. Spectrosc. 198, 218-229 (1999).
14. V. Zeninari, B. Parvitte, D. Courtois, N.N. Lavrentieva, Yu. N. Ponomarev, G. Durry, Mol. Phys. 102, 1697-1706 (2004).
15. A.D. Bykov, N.N. Lavrentieva, T.P. Mishina, L.N. Sinitsa, R.J. Barber, R.N.

Tolchenov, J. Tennyson, J. Quant. Spectrosc. Radiat. Transfer 109, 1834-1844 (2008).

16. J.T. Hodges, D. Lisak, N. Lavrentieva, A. Bykov, L. Sinitsa, J. Tennyson, R.J. Barber, R.N. Tolchenov, J. Mol. Spectrosc. 249, 86-94 (2008).
17. A.D. Bykov, N.N. Lavrentieva, T.M. Petrova, L.N. Sinitsa, A.M. Solodov, R.J. Barber, J. Tennyson, R.N. Tolchenov, Optika i spectroscop. 105, 25-31 (2008).
18. N. Lavrentieva, A. Osipova, L. Sinitsa, Ch. Claveau, A. Valentin, Mol. Phys. 106, 1261-1266 (2008).
19. N.N. Lavrentieva, T.P. Mishina, L.N. Sinitsa, J. Tennyson, Atm. Oceanic Opt. 21, 1096-1100 (2008).
20. S.A. Tashkun, V.I. Perevalov, J.-L. Teffo, A.D. Bykov, N.N. Lavrentieva, CDSD-1000, J. Quant. Spectrosc. Radiat. Transfer 82, 165-196 (2003).
21. ftp://ftp.iao.ru/pub/CDSD-1000.
22. http://saga.atmos.iao.ru.
23. C.J. Tsao, B. Curnutte, J. Quant. Spectrosc. Radiat. Transfer 2, 41-91 (1962).
24. R.P. Leavitte, J. Chem. Phys. 73, 5432-5450 (1980).
25. A. Bykov, N. Lavrent'eva, and L. Sinitsa, Opt. Spektrosk. 83, 73-82 (1997).
26. A.D. Bykov, N.N. Lavrentieva, Atm. Opt. 4, 518-529 (1991).
27. K.M. Mack, J.S. Muenter, J. Chem. Phys. 66, 5278-5283 (1977).
28. A.Yu. Stepukhin, V.A. Udovenya, L.S. Kostyuchenko, Izv. Vyssh. Uch. Zaved. SSSR, Fizika, Dep. VINITI, No. 2182-B91 (1991).
29. C.H. Townes and A.L. Schawlow, Microwave spectroscopy, McGraw-Hill, New York, NY, 1955.
30. L.D. Landau and E.M. Lifshitz, Quantum Mechanics, Pergamon Press, New York, 1965.
31. P. Varanasi, J. Quant. Spectrosc. Radiat. Transfer 39, 13-25 (1988).

32. G. Wagner, M. Birk, R.R. Gamache, and J.M. Hartmann, J. Quant. Spectrosc. Radiat. Transfer 92, 211-230 (2005).

33. R.A. Toth, L.R. Brown, MA.H. Smith, V. M. Devi, D. C. Benner, M. Dulick, J. Quant. Spectrosc. Radiat. Transfer 101, 339-366 (2006).

34. R.R. Gamache and L.S. Rothman, Abstracts of the Xth Colloquium on High Resolution Molecular Spectroscopy, Dijon, 14-18 September 1987, p. 288.

35. H.M. Pickett, J. Chem. Phys. 73, 6090 (1980).

Table 1. Molecular and spectroscopic constants used in calculations.

	O_3	N_2	O_2
μ, D	-0.532	0	0
Q, D Å	Q_{xx} = -1.4	1.4	0.4
	Q_{yy} = -0.7		
	Q_{zz} = 2.1		
α, Å^3	α_i = 2.8	1.76	1.59
	α_i^{xx} =2.0		
	α_i^{yy} =1.8		
	α_i^{zz} = 4.6		
	α_f = 2.89 (101)		
	α_f^{zz} = 5.14 (101)		
	α_f = 2.85 (200)		
	α_f^{zz} = 5.01 (200)		
	α_f = 2.88 (002)		
	α_f^{zz} = 4.68 (002)		
I, 10^{-25}erg	2.126	2.485	2.003
B_0, cm^{-1}	-	1.998	1.4456
D_0, cm^{-1}	-	$5.76\cdot10^{-6}$	$4.839\cdot10^{-6}$

Table 2. Calculated and experimental [5] O_3-N_2(O_2) line shift coefficients δ (10^{-3} $cm^{-1}atm^{-1}$) and temperature exponents N for the $\nu_1+\nu_3$ band. **Lines used for fitting are marked with asterisk.**

J'	K_a'	K_c'	J	K_a	K_c	O_3-N_2			O_3-O_2	
						δ calc.	δ expt	N calc.	δ calc.	δ expt
42	2	41	43	2	42	-3.28	-4.2	0.78	-4.54	-5.3
38*	5	34	39	5	35	-3.25	-4.0	0.94	-4.69	-4.8
37	4	33	38	4	34	-2.60	-4.0	1.10	-3.73	-4.4
34	6	29	35	6	30	-3.37	-3.6	1.10	-4.71	-4.9
32	5	28	33	5	29	-2.92	-3.3	1.06	-4.22	-4.3
31	6	25	32	6	26	-3.27	-3.6	1.10	-4.53	-4.3
31	5	26	32	5	27	-2.80	-2.7	1.12	-3.99	-3.7
31	1	30	32	1	31	-2.85	-3.8	0.83	-4.06	-4.5
30	5	26	31	5	27	-2.86	-3.7	1.09	-4.15	-4.3
31	0	31	32	0	32	-3.52	-4.4	0.74	-4.76	-4.7
30	1	30	31	1	31	-3.50	-4.2	0.74	-4.76	-4.5
28	6	23	29	6	24	-3.14	-3.5	1.10	-4.37	-3.9
29	0	29	30	0	30	-3.48	-3.2	0.75	-4.72	-4.7
27	6	21	28	6	22	-3.11	-3.0	1.10	-4.33	-3.8
28	2	27	29	2	28	-2.89	-3.5	0.88	-4.12	-4.2
28	1	28	29	1	29	-3.46	-3.1	0.76	-4.71	-4.2
27	1	26	28	1	27	-2.66	-3.3	0.87	-3.82	-4.0
27*	0	27	28	0	28	-3.43	-3.3	0.75	-4.66	-3.8
25	5	20	26	5	21	-2.88	-3.0	1.15	-4.13	-3.4
25	3	22	26	3	23	-2.17	-2.9	1.08	-3.26	-3.5
24	6	19	25	6	20	-3.01	-3.0	1.10	-4.27	-3.3
25	1	24	26	1	25	-2.58	-3.1	0.90	-3.72	-4.0
24	5	20	25	5	21	-2.80	-3.0	1.13	-4.03	-3.5
24	4	21	25	4	22	-2.62	-3.2	1.05	-3.87	-4.0
23	6	17	24	6	18	-2.98	-2.4	1.11	-4.26	-3.5
22*	8	15	23	8	16	-3.24	-3.2	1.04	-4.68	-3.3
23	5	18	24	5	19	-2.78	-2.8	1.13	-4.01	-3.6
22	7	16	23	7	17	-3.14	-2.8	1.07	-4.52	-3.6
23	4	19	24	4	20	-2.38	-2.9	1.13	-3.53	-3.4
22	5	18	23	5	19	-2.73	-3.2	1.12	-3.95	-3.9
21	7	14	22	7	15	-3.10	-3.1	1.06	-4.49	-3.4
23	0	23	24	0	24	-3.27	-3.1	0.79	-4.56	-4.0
20	8	13	21	8	14	-3.14	-3.0	1.02	-4.45	-3.4
20	7	14	21	7	15	-3.06	-3.1	1.05	-4.41	-3.4
19	7	12	20	7	13	-3.02	-2.4	1.04	-3.37	-3.5
14	3	12	15	3	13	-2.25	-2.1	1.01	-3.45	-2.6
10	4	7	11	4	8	-2.28	-1.8	0.99	-3.39	-2.4
8	4	5	9	4	6	-2.25	-2.2	0.94	-3.36	-2.5
3*	2	1	2	2	0	-2.39	-2.0	0.81	-4.66	-1.2
27	0	27	26	0	26	-3.43	—	0.75	-4.53	-3.0
37	6	31	36	6	30	-3.26	—	1.09	-4.01	-3.3
37	2	35	36	2	34	-2.74	-3.2	1.03	-4.54	-3.9

Table 3. Statistics for $\Delta = |\delta^{expt} - \delta^{calc.}|$ values.

Δ, 10^{-3} $cm^{-1}atm^{-1}$	Percentage of lines	
	O_3-N_2	O_3-O_2
$\Delta \leq 1$	98%	87%
$1 < \Delta \leq 2$	2%	11%
$2 < \Delta \leq 3$	–	–
$3 < \Delta$	–	2%

Table 4. Calculated and experimental [6] O_3-N_2 line shift coefficients for the $2\nu_1$ band (10^{-3} $cm^{-1}atm^{-1}$). **Lines used for fitting are marked with asterisk.**

J'	K_a'	K_c'	J	K_a	K_c	calc.	expt
25*	6	20	26	7	19	-2.23	-1.9
28	5	23	29	6	24	-2.37	-1.7
14	7	7	15	8	8	-1.71	-1.8
28	4	24	29	5	25	-2.92	-1.5
24	4	20	25	5	21	-2.57	-1.7
29	3	27	30	4	26	-1.12	-1.2
13*	3	11	14	4	10	-2.11	-2.8
43*	1	43	44	0	44	-2.56	-2.5
42	0	42	43	1	43	-2.56	-3.4
18	2	16	19	3	17	-2.60	-2.4
32	0	32	33	1	33	-2.34	-2.2
37	4	34	38	3	35	-0.89	-1.7
25	1	25	26	0	26	-2.13	-1.2
25	2	24	26	1	25	-1.32	-2.7
17	1	17	18	0	18	-1.85	-2.1
12	0	12	13	1	13	-2.52	-1.7
15	2	14	16	1	15	0.04	-2.3

Table 5. Calculated and experimental [6] O_3-N_2 line shift coefficients for the $2\nu_3$ band (10^{-3} $cm^{-1}atm^{-1}$). **Lines used for fitting are marked with asterisk.**

J'	K_a'	K_c'	J	K_a	K_c	calc.	expt
8*	8	0	9	9	1	-3.95	-4.8
21*	8	14	21	9	13	-6.31	-7.0
26	6	20	26	7	19	-6.20	-6.2
18	6	12	18	7	11	-5.68	-5.2

Figure captions

Figure 1. Calculated and experimental [5] O_3-N_2 line shifting coefficients for the $\nu_1+\nu_3$ band. **The usual abscissa *J* is incremented by 0.1K_a in order to separate the transitions with identical *J* but different K_a values.**

Figure 2. Calculated and experimental [6] O_3-N_2 line shifting coefficients for the $2\nu_1$ band. **The usual abscissa *J* is incremented by 0.1K_a in order to separate the transitions with identical *J* but different K_a values.**

Figure 3. Calculated temperature dependence of the nitrogen-induced 25 5 20 ← 26 5 21 line shift in the $\nu_1+\nu_3$ band (upper panel) and the corresponding plot in logarithmic coordinates used to deduce the *N* value (lower panel).

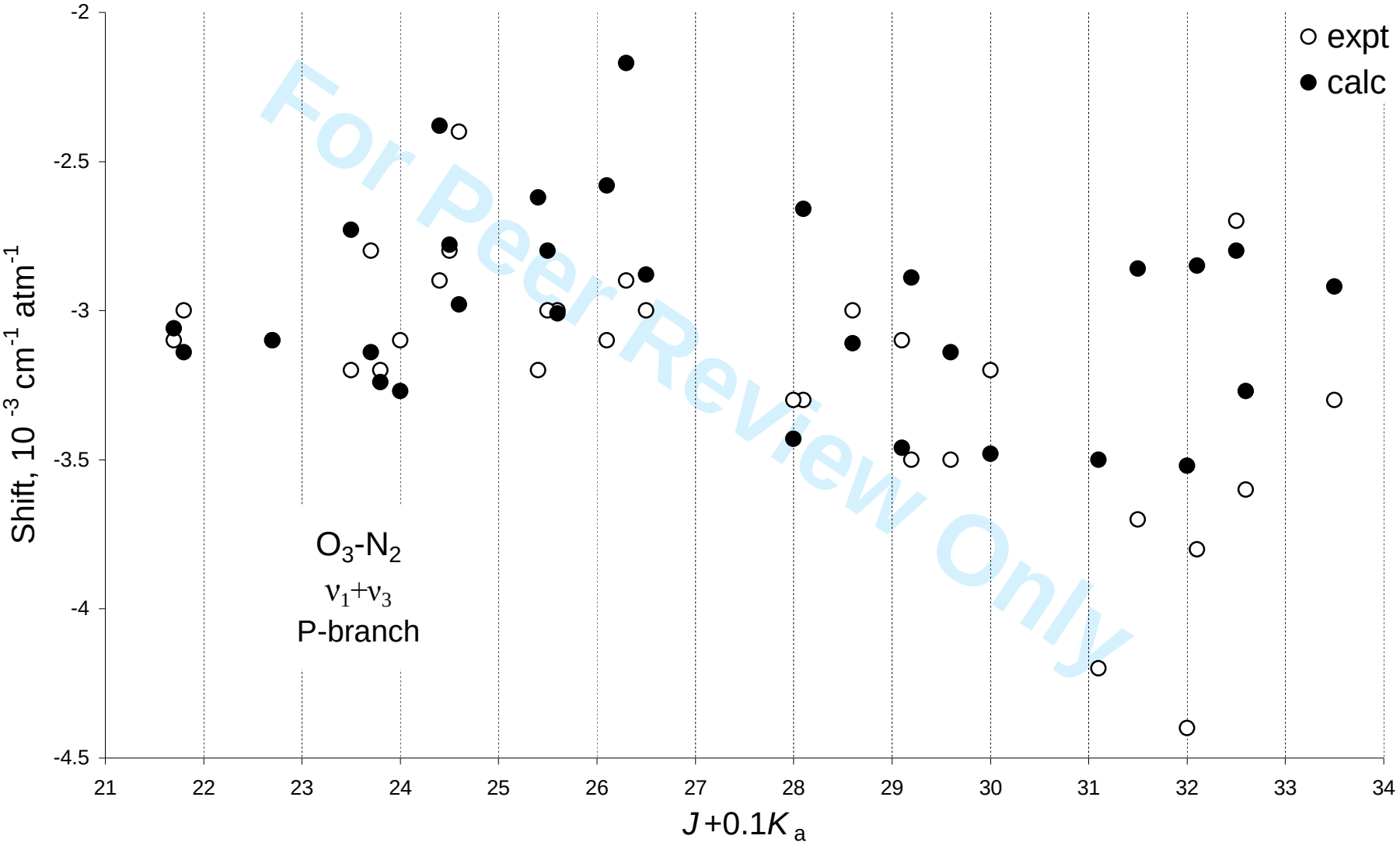

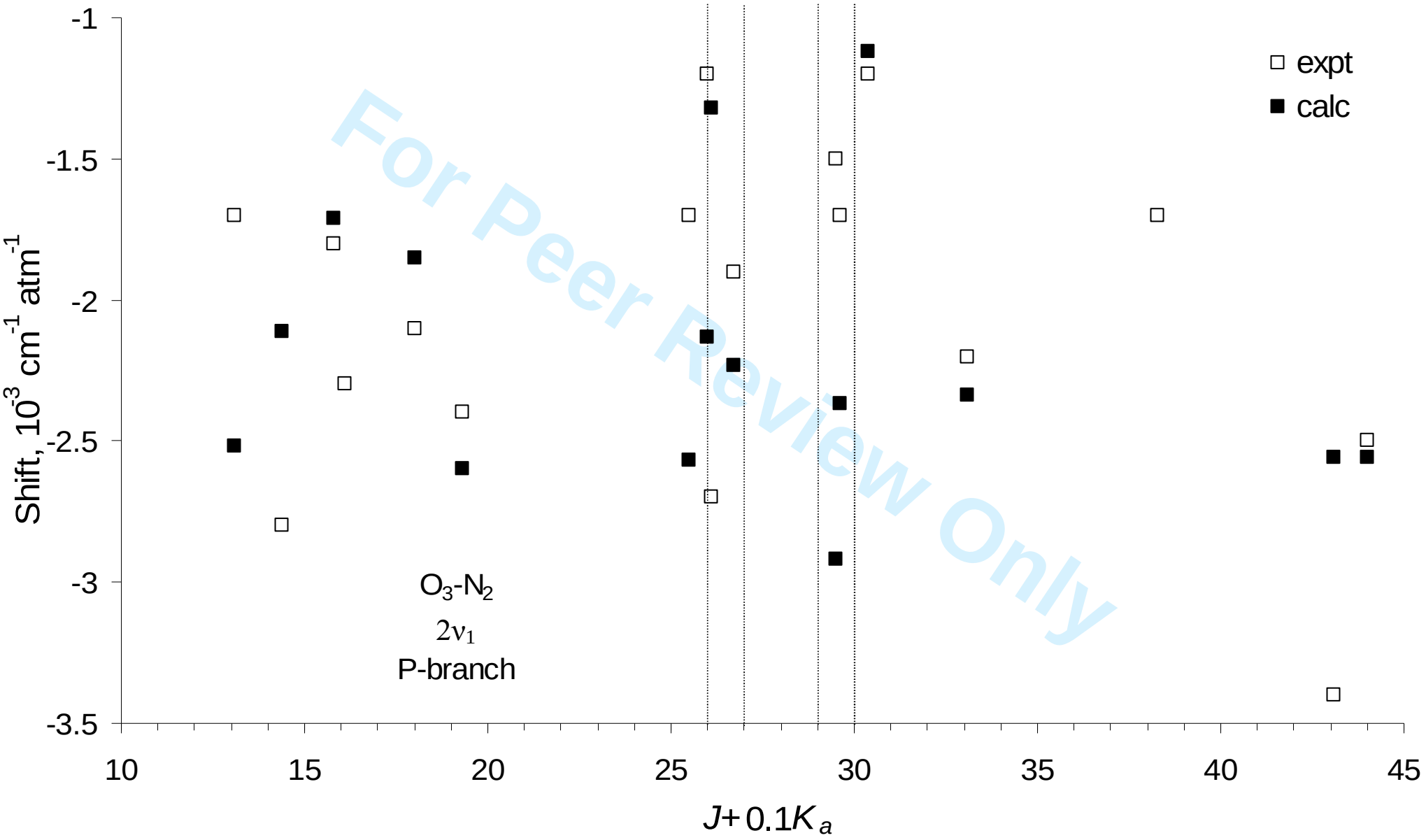

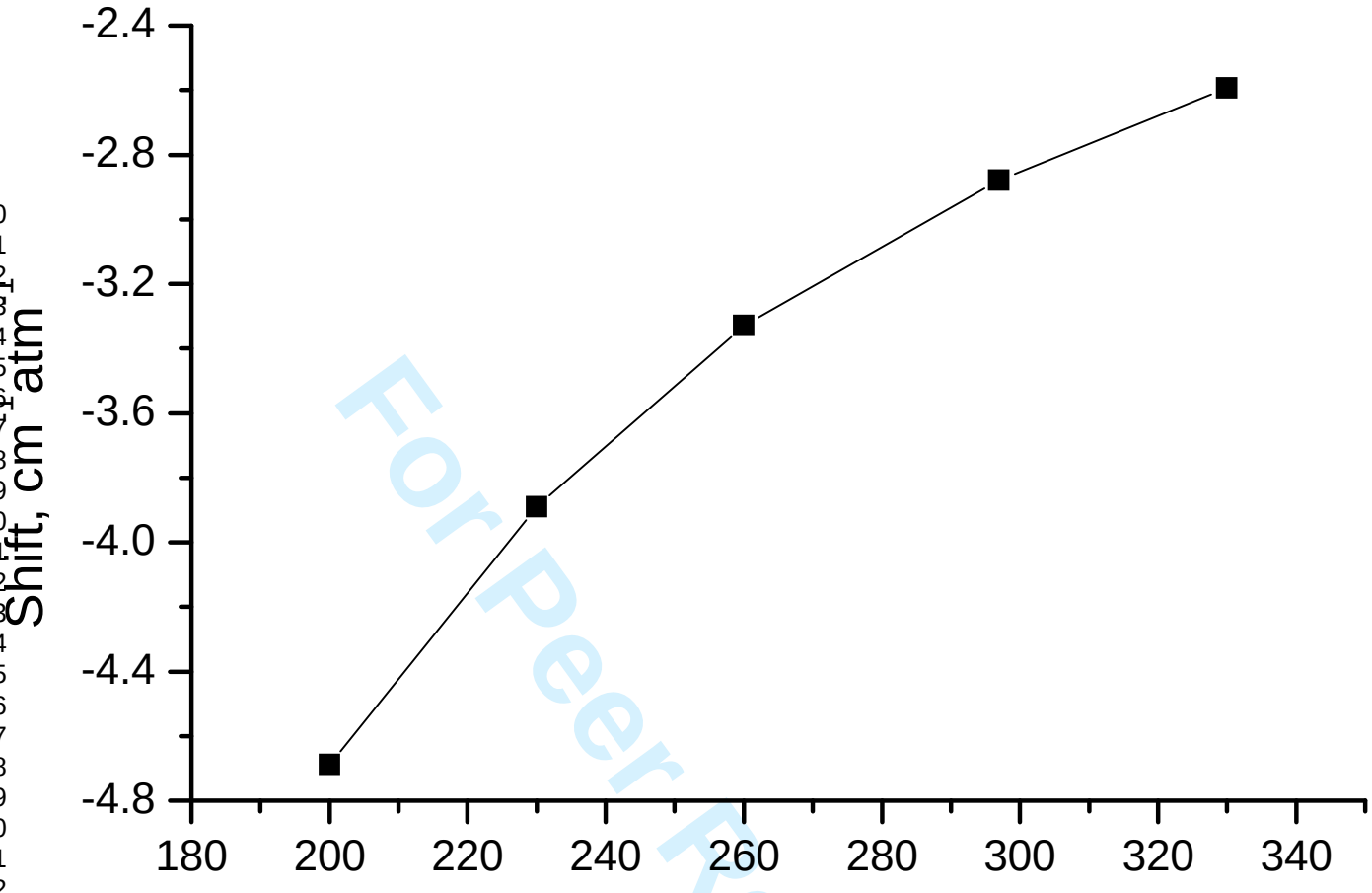

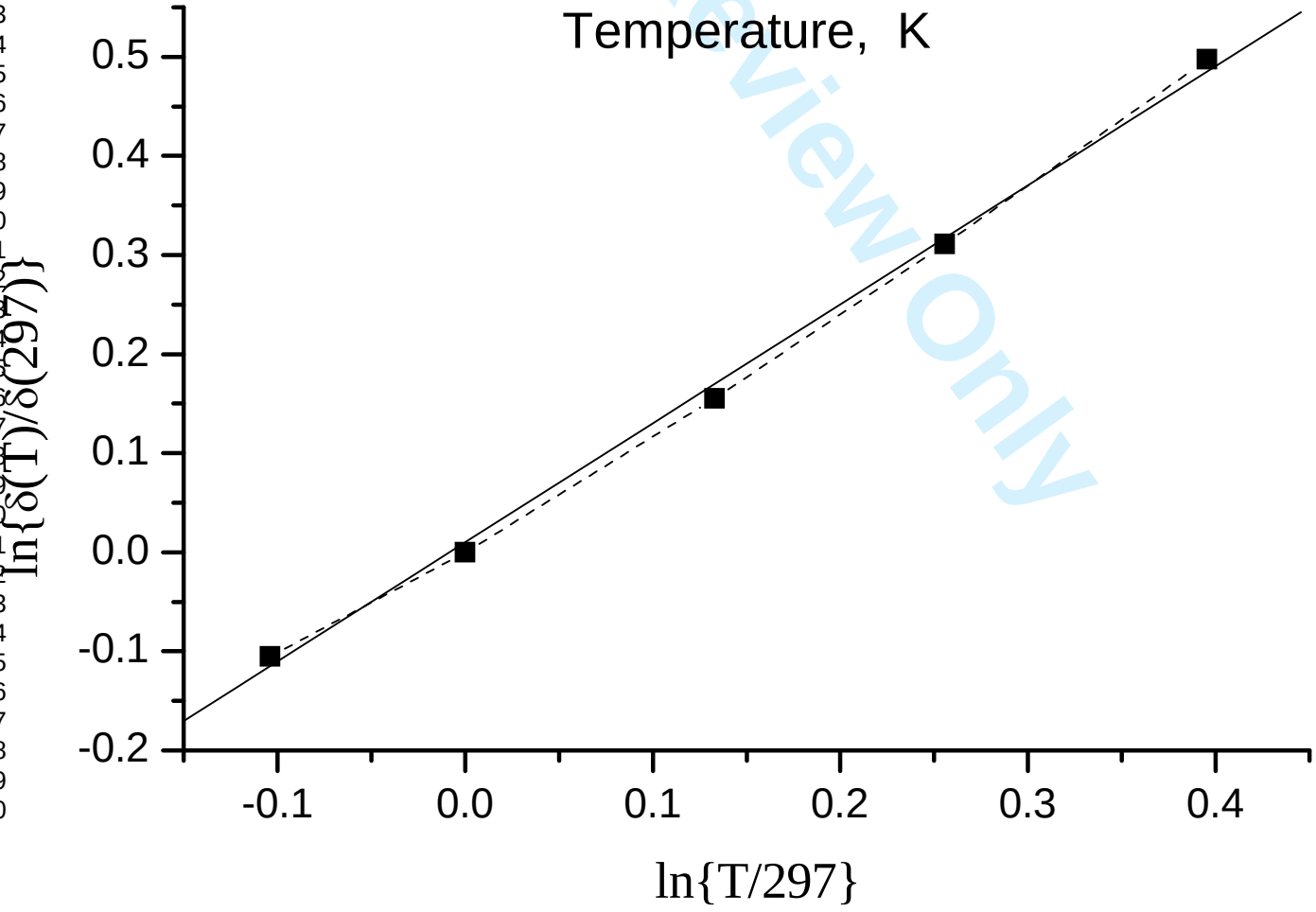

Calculations of ozone line shifting induced by N_2 and O_2 pressure

N. Lavrentieva [a], A. Osipova [b] and J. Buldyreva [c*]

[a] Institute of Atmospheric Optics, 1 ave Akademicheskii, 634055 Tomsk, Russia

[b] Tomsk State University, 36 ave Lenina, 634050, Tomsk, Russia

[c] Institut UTINAM, UMR CNRS 6213, Université de Franche-Comté, 16 route de Gray, 25030 Besançon cedex, France

[*] Corresponding author ; Phone: +33 (0)3 81 66 63 60; FAX: +33 (0)3 81 66 64 75; Electronic address : jeanna.buldyreva@univ-fcomte.fr

Abstract

Ozone line shifts by nitrogen and oxygen pressure are computed for the $\nu_1+\nu_3$, $2\nu_1$ and $2\nu_3$ bands of the 5μm spectral region by a semiempirical approach. The calculated values agree with measurements better than 0.001 $cm^{-1}atm^{-1}$ for 98% of O_3-N_2 lines and 87% of O_3-O_2 lines. In contrast with the water molecule case, the polarization components of the interaction potential are shown to contribute to the line shift more efficiently than the electrostatic interactions. As intermediate results, the mean dipole polarizability and the components of the polarizability tensor for the vibrational states (101), (200), and (002) of ozone molecule are determined by least-squares fitting of theoretical shifts to some experimental values. The temperature exponents for the $\nu_1+\nu_3$ band lines are also estimated.

Keywords: ozone, line shift, semiempirical calculation, polarizability in excited vibrational state, temperature exponent

I. Introduction

Among the minor constituents of the Earth's atmosphere ozone receives a particular attention of scientists due to its double role of protector and pollutant: whereas the stratospheric ozone layer protects the humans, animals and vegetation from the harmful ultraviolet radiation of the Sun, the excessive concentration of ozone in the troposphere is qualified as pollution because of its toxic effects for respiration. Precise measurements of vertical ozone concentration profiles are therefore of crucial importance for health protection services and scientific community interested in comprehension and global modelling of the terrestrial atmosphere.

The probing of atmospheric species is principally realized by non intrusive spectroscopic techniques in the infrared, microwave and millimeter domains. For ozone, the spectral regions of 5 µm and 10 µm are of particular interest since they correspond simultaneously to its most intense absorption bands and to "atmospheric windows" free of water vapour absorption. Reliable inversion of the recorded spectra requires a precise knowledge of ozone spectral line shape parameters (including its main isotopic species) in a wide temperature range and in different vibrational bands.

While the ozone line broadening has been quite intensively studied both experimentally and theoretically, its line shifting data remain quite sparse. Only some measurements were made by Smith et al. [1-4], Barbe et al. [5-6] and Sokabe et al. [7] and only QFT (Quantum Fourier Transform) and ATC (Anderson-Tsao-Curnutte) calculations were realized by Gamache and co-workers [8-9] for N_2, O_2 and air-broadening. Recently, the complex-valued version of the Robert-Bonamy formalism was employed by Drouin et al. [10] to estimate line shifts induced by the same perturbers in the rotational band of O_3; no experimental data were reported however for comparison because of their too small values. From the theoretical point of view the line shifting mechanism has a more

complicated character than the line broadening, and many factors negligible for the width become important for the shift (strong dependencies on vibrational quantum numbers, type of perturbing molecules, isotopic species). Since the pressure shift is more sensitive to the intermolecular interaction details than the line broadening, it represents a very promising tool for molecular collision studies. An exhaustive analysis of available experimental data and calculation of line shifts induced in particular by nitrogen and oxygen are therefore of great importance for better understanding of the shifting mechanism and improvement of our knowledge of the ozone spectroscopic properties.

In this paper we present a first systematic calculation of O_3-$N_2(O_2)$ vibrotational line shifting coefficients and of their temperature dependence for three vibrational bands of the 5μm region ($\nu_1+\nu_3$, $2\nu_1$, $2\nu_3$) by a semiempirical method developed previously [11] and successfully applied to the case of O_3-$N_2(O_2)$ line broadening [12]. In the frame of this approach the impact theory is modified by introducing additional semiempirical parameters determined by fitting to experimental data. They are used further to calculate the line shifts which have been not measured. This method gives the possibility to calculate separately the contributions to the line shape parameters from different types of intermolecular interactions and from different scattering channels, which enables an analysis of vibration-rotational dependence of the shifting coefficients for various kinds of perturbers.

II. Method of calculation

The semiempirical method [11] has been already used for calculation of line shape parameters and their temperature exponents for H_2O-N_2, H_2O-O_2, H_2O-H_2O_2, CO_2-N_2 and CO_2-O_2 molecular systems [13-20]. In Refs [13-19] it has been shown that for polar active molecules the semiempirical approach gives quite accurate parameters values. The results of these calculations are actually included in a freely-available carbon dioxide spectroscopic data bank [21] and in the “ATMOS” Information System [22].

In the framework of this approach the line shift corresponding to the radiative transition from the initial state i to the final state f depends on the transition probabilities $D^2(ii'|l)$ and $D^2(ff'|l)$ of the different scattering channels connecting the levels i and f with their neighbouring levels:

$$\delta_{if} = B(i,f) + \sum_{l,i'} D^2\left(ii'\middle|l\right)P_l\left(\omega_{ii'}\right) + \sum_{l,f'} D^2\left(ff'\middle|l\right)P_l\left(\omega_{ff'}\right) + \ldots \qquad (1)$$

(the higher order terms are neglected). These transition probabilities represent the squared reduced matrix elements of the relevant molecular operators such as the components of the dipole moment (tensorial order l = 1), the components of the quadrupole tensor (l = 2) or the components of higher multipoles. The expansion coefficients $P_l(\omega)$, called in the literature "interruption" or "efficiency functions", depend on the intermolecular potential, the trajectory, the energy levels and the wave functions of the perturbing molecule. They can be seen as interruption functions for a given scattering channel and can be formally written as a product of the interruption function of the ATC theory $P_l^{ATC}(\omega)$ and of a correction factor $C_l(\omega)$ deduced from fitting to experimental data:

$$P_l(\omega) = C_l(\omega)P_l^{ATC}(\omega). \qquad (2)$$

In order to account for the rotational dependence of the interruption function the form of this correction factor is chosen as

$$C_l(\omega) = \frac{c_1}{c_2\sqrt{J}+1} \quad , \qquad (3)$$

where the fitting parameters c_1 and c_2 are responsible respectively for the correction of errors induced by the cut-off procedure and the vibrational dependence. These parameters values c_1 = 2.7 and c_2 = 7.0 were taken from our previous work [12] on the ν_1+ν_3 band line broadening coefficients (fitting to some experimental values from R- and P-branches with various values of the rotational quantum number J) and used here for three considered vibrational bands without any change. This fact confirms the internal consistency of the

semiempirical approach for simultaneous prediction of both line widths and line shifts.

The first term $B(i, f)$ appearing in Eq. (1) accounts for the contribution of the isotropic part of the interaction potential:

$$B(i,f) = \frac{n}{c} B_1 \left[\alpha_2 (\mu_f^2 - \mu_i^2) + \frac{3 I I_2 (\alpha_f - \alpha_i)}{2(I + I_2)} \right] \sum_p \rho(p) \int_0^\infty v F(v) b_0^{-3}(v, p, i, f) dv \,, \qquad (4)$$

where n is the number density of the perturbing molecules and ρ is the population of their different (rotational) states p, the constant $B_1 = -3\pi/(8\hbar v)$, and $\alpha\,(\alpha_2)$, μ, $I\,(I_2)$ are, respectively, the mean polarizability, dipole moment, and ionization potential of the active (perturbing) molecule. The integration on the relative molecular velocity v is made with the Maxwell-Boltzmann distribution function $F(v)$ and b_0 means the interrupting radius. In the excited vibrational states the mean dipole polarizability is not well known whereas through Eq. (4) it is responsible for the (very clearly pronounced) vibrational dependence of the line shifting coefficient. In our calculations we therefore considered it as an additional fitting parameter.

Equation (1) for the line shift can be expressed in terms of the conventional ATC interruption functions $S_1(b)$ and $S_2(b)$ which depend on the impact parameter b and correspond to the contributions from the isotropic and anisotropic parts of the interaction potential, so that

$$S_1(b) = B(i, f), \qquad (5)$$

$$S_2(b) = \sum_{l,i'} D^2(ii'|l) P_l(\omega_{ii'}) + \sum_{l,f'} D^2(ff'|l) P_l(\omega_{ff'}) \,. \qquad (6)$$

For O_3-$N_2(O_2)$ case the $S_2(b)$ contribution can be written as

$$S_2(b) = S_2^{12e}(b) + S_2^{22e}(b) + S_2^{22p}(b) + S_2^{02p}(b) + S_2^{20p}(b) \,, \qquad (7)$$

where the numerical superscripts denote the multipolarity of the interactions for the active and perturbing molecules and the superscripts e and p denote respectively the electrostatic

and the polarization parts of the interaction potential. Namely, the terms $S_2^{12e}(b)$ and $S_2^{22e}(b)$ come from the dipole-quadrupole and quadrupole-quadrupole interactions whereas the terms $S_2^{22p}(b)$, $S_2^{02p}(b)$ and $S_2^{20p}(b)$ are due to the polarization and dispersion contributions. Their detailed expressions can be found in [23, 24]. According to Eq. (4) the interruption function $S_1(b)$ related to the isotropic potential is determined by $\mu_f^2 - \mu_i^2$ and $\alpha_f - \alpha_i$ differences. The terms $S_2^{22p}(b)$, $S_2^{02p}(b)$ and $S_2^{20p}(b)$ depend on $\alpha_i - \alpha_i^{zz}$, $\alpha_f - \alpha_f^{zz}$, $\alpha_i^{xx} - \alpha_i^{yy}$, and $\alpha_f^{xx} - \alpha_f^{yy}$ values, where $\alpha_{i(f)}^{xx}$, $\alpha_{i(f)}^{yy}$, $\alpha_{i(f)}^{zz}$ are the Cartesian components of the polarizability tensor of the absorbing molecule in the initial (final) states.

In [25] it has been shown that the vibrational dependence of the line shift coefficients of water vapour is explained by the intermolecular potential: the shift is mainly determined by the polarization term $S_1(b)$ and the electrostatic term $S_2^{12e}(b)$. In contrast with the water vapour molecule, the ozone molecule has a three times smaller dipole moment (0.53 D) while a two times greater mean polarizability (2.8 Å^3) in the fundamental vibrational state. Therefore for O_3-$N_2(O_2)$ interactions the second-order polarization contributions $S_2^{22p}(b)$, $S_2^{02p}(b)$ and $S_2^{20p}(b)$ are expected to be significant, and in addition to the electrostatic terms we accounted in our calculations for the interactions like dipole-induced dipole. The polarization contributions to $S_2(b)$ were calculated using the resonance functions Ig_1 and Ig_2 determined earlier in [26].

In the present study we have determined the components of the polarizability tensor of the ozone molecule responsible for induction and dispersive interactions. The components for the ground vibrational state were measured in [27] and calculated in [28], the first derivatives of the polarizability with respect to the normal coordinates were also determined, but not the second derivatives necessary for estimating the polarizability in the

excited states. For our purposes, the polarizability in the upper vibrational state α_f and the α_f^{zz} component of the polarizability tensor were obtained by least-squares fitting to several experimental line shifts induced by nitrogen pressure, for each band separately. Since the *xx*- and *yy*-components have close values, the difference $\alpha_f^{xx} - \alpha_f^{yy}$ was taken equal to its ground vibrational state value. The adjusted parameters α_f and α_f^{zz} were further used to calculate the line shifts due to oxygen pressure. Table 1 gathers molecular and spectroscopic constants for ozone, nitrogen and oxygen used in our calculations.

III. Results and discussion

For the $\nu_1+\nu_3$ band (J = 2–43) calculated O_3-$N_2(O_2)$ line shift coefficients are presented in Table 2 **(lines used for fitting are marked with asterisk)** together with the corresponding experimental values from Ref. [5]. These measurements were obtained with the spectral resolution of 0.002 cm^{-1} and the accuracy of the line shift coefficients estimated at $2.5 \cdot 10^{-4} cm^{-1} atm^{-1}$ (12%) for most lines ($15 \le J \le 30$, $K_a \le 6$) and at $4 \cdot 10^{-4} cm^{-1} atm^{-1}$ for other lines ($J < 15$, $J > 30$, $K_a > 6$). It is clearly seen from this table that the line shifts by collisions with oxygen molecules are greater than those by collisions with nitrogen molecules. This fact is due to an increasing contribution from $S_1(b)$ (which is always negative) with decreasing interrupting radius b_0. By the way, it leads to the corresponding decrease of the broadening coefficients. Comparison of calculated values with experimental data shows a very good agreement between them: the difference $\Delta = |\delta^{expt} - \delta^{calc.}|$ does not exceed 0.001 cm^{-1} atm^{-1} for 98% of O_3-N_2 lines and 87% of O_3-O_2 lines with the standard deviation of $7.04 \cdot 10^{-5}$ $cm^{-1} atm^{-1}$. The details of statistics are given in Table 3.

The K_a-dependence of the $\nu_1+\nu_3$ band transitions can be seen on Fig. 1 where a specific combination of the quantum numbers (J + 0.1K_a) allows separation of the

lines with identical *J*-values but different K_a-values (the *J*-interval starts with *J*=21 for which K_a=7 and K_a=8 are available). As can be seen from this figure, for some high *J* values (*J* = 26, 31, 32) the calculation reproduces correctly the general behaviour of the experimental K_a-dependences (line shift increases and then decreases with K_a increasing). It is not however the case for other values of *J* because of the semiempirical character of our model: fitting to some arbitrary chosen experimental values allows a global minimisation of deviations from experimental points but not reproducing fine details in K_a-dependences.

To analyze the vibrational dependence of shifting coefficients, in addition to the band $\nu_1+\nu_3$ two other bands $2\nu_1$ and $2\nu_3$ were studied for the case of nitrogen broadening. Our theoretical and experimental [6] values for these **two bands are given in Tables 4-5.** The general comparison of the results for three studied bands shows that the (absolute) line shifts for $2\nu_1$ band are smaller than those of $\nu_1+\nu_3$ and $2\nu_3$ bands. Indeed, because of the strong polarizability of the ozone molecule the shift becomes noticeable already for transitions to low vibrational states and increases even more for higher vibrational frequencies. A strong vibrational effect and a rotational dependence thus should be noted for the ozone line shifting coefficients. **It is difficult to analyse the K_a-dependence for these bands since only in the $2\nu_1$ band and only for two *J*-values (*J* = 26, 29) a couple of various K_a values (K_a =0, 1 and K_a =5, 6, respectively) are available. As shows Fig. 2, for these *J*-values the experimental shifts decrease whereas the calculated shifts increase when passing from K_a =0 (or K_a =5) to K_a =1 (or K_a =6), which can be explained again by the semiempirical character of our approach.**

An additional point of our work consisted in evaluation of the temperature dependence of line shifts. The temperature exponents *N* were determined using the relation

$$\delta_{if}(T) = \delta_{if}(297)\left(\frac{T}{297}\right)^{-N}, \qquad (8)$$

where $\delta_{if}(297)$ is the shift value at the reference temperature 297 K. This kind of relation is widely used in the literature and in HITRAN database to characterise the temperature dependence of the line widths, but mainly for historical reasons since it is valid for molecules interacting through a potential $r^{-\eta}$ [29–31] and can lead to negative values of the temperature exponents for certain transitions of H_2O perturbed by nitrogen, oxygen or air [32, 33]; for rotational transitions of O_3 perturbed by air this relation was found to be correct for the temperature range 225-350 K but not for the 150-450 K [10]. For the line shifts this relation works well [18] when the shift behaviour with temperature variation is quite regular (Eq. (8) does not describe a change of sign). It is the case for the shifts considered in the present paper. We note for completeness, that a similar formula for the line shift temperature dependence was proposed by Gamache and Rothman [34] which introduces a temperature-dependent sign but is not zero at intermediate temperatures; for our case their expression is equivalent to Eq. (8).

Line shift calculations were carried out for five temperatures (200, 230, 260, 297 and 330 K), and the corresponding N values were extracted by a least-squares fitting procedure. For all studied lines the standard deviation did not exceed 10^{-6} $cm^{-1}atm^{-1}$. **Figure 3 shows an example of temperature dependence for the shift of the line 25 5 20 ← 26 5 21 from the $\nu_1+\nu_3$ band (upper panel) and the corresponding plot in logarithmic coordinates (lower panel). The practically linear dependence of $\ln\{\delta(T)/\delta(297)\}$ on $\ln(T/297)$ confirms the validity of Eq. (8) for the temperature dependence of line shifts. For the $\nu_1+\nu_3$ band of O_3-N_2 system the temperature exponent values are given in Table 2.** As can be seen from this table, N varies slightly from 0.74 to 1.15 for the lines with J = 9 - 43, with the mean value equal to 0.986. It should be noted that these calculations refer to the lines with $\Delta K_a = 0$ and $\Delta K_c = 1$ (for other transitions the temperature exponent values can be in principle quite different).

A very rough theoretical estimation of the temperature exponent values for Eq. (8)

can be made with the formula obtained by Pickett [35]:

$$N = 1 + \frac{3}{2\eta - 2}, \tag{9}$$

which gives N =1.5 for the dipole-quadrupole (η = 4) and N =1.375 for quadrupole-quadrupole (η = 5) interactions. Our results are therefore quite consistent with these estimations.

IV. Conclusions

The comparison of our calculations with experimental values argues that the semiempirical method is quite acceptable for estimating the shifts of ozone vibrotational absorption lines. For this molecule the polarization components of the interaction potential are shown to contribute to the line shift more effectively than the electrostatic dipole-quadrupole interaction (which is very significant for the line broadening). Whereas for the ozone line broadening by nitrogen and oxygen the vibrational effects are very weak, its line shifts demonstrate a strong vibrational dependence. For accurate calculation of ozone line shift coefficients it is therefore necessary to account for this dependence in some components of the ozone polarizability tensor and its polarizability in the excited vibrational states. These components are determined in the present work for (101), (200) and (002) vibrational states by fitting to experimental data. The temperature dependence of the line shifting coefficients is additionally studied. In general, the mechanisms responsible for the ozone line shifting appear to be much more complex than those responsible for the line broadening, which should be permanently kept in mind when calculating its line shape parameters.

The calculated values are intended for use in spectroscopic databases, for example, the "ATMOS" Information System (http://saga.atmos.iao.ru).

Acknowledgements

The authors acknowledge the financial support by the French national program LEFE-CHAT and by the program "Optical Spectroscopy and Frequency Standards" of the Russian Academy of Sciences.

References

1. M.A.H. Smith, C.P. Rinsland, V. M. Devi, D.C. Benner, and K.B. Thakur, J. Opt. Soc. Am. B 5, 585-592 (1988).
2. M.A.H. Smith, C.P. Rinsland, V. Malathy Devi, E.S. Prochaska, J. Mol. Spectrosc. 164, 239-259 (1994); Erratum, J. Mol. Spectrosc. 165, 596 (1994).
3. M.A.H. Smith, V. Malathy Devi, D.C. Benner, C.P. Rinsland, J. Mol. Spectrosc. 182 (1997) 239-259.
4. V. Malathy Devi, D.C. Benner, M.A.H. Smith, C.P. Rinsland, J. Mol. Spectrosc. 182, 221-238 (1997).
5. A. Barbe, S. Bouazza, J.J. Plateaux, Appl. Opt. 30, 2431-2436 (1991).
6. A. Barbe, J.J. Plateaux, S. Bouazza, Proceedings of the Tenth All-Union Symposium on High Resolution Molecular Spectroscopy, SPIE 1811, Washington, USA, 83-102 (1991).
7. N. Sokabe, M. Hammerich, T. Pedersen, A. Olafsson, J. Henningsen, J. Mol. Spectrosc. 152, 420-433 (1992).
8. R.R. Gamache, L.S. Rothman, Appl. Opt. 24, 1651-1656 (1985).
9. R.R. Gamache, R.W. Davies, J. Mol. Spectrosc. 109, 283-299 (1985).
10. B. J. Drouin, J. Fischer, R.R. Gamache, J. Quant. Spectrosc. Radiat. Transfer 83, 63-81 (2004).
11. A. Bykov, N. Lavrentieva, L. Sinitsa, Mol. Phys. 102, 1653-1658 (2004).
12. J. Buldyreva, N. Lavrentieva, Mol. Phys. 2009 (in press).
13. A. Valentin, Ch. Claveau, A. Bykov, N. Lavrentieva, V. Saveliev, L. Sinitsa, J. Mol. Spectrosc. 198, 218-229 (1999).
14. V. Zeninari, B. Parvitte, D. Courtois, N.N. Lavrentieva, Yu. N. Ponomarev, G. Durry, Mol. Phys. 102, 1697-1706 (2004).
15. A.D. Bykov, N.N. Lavrentieva, T.P. Mishina, L.N. Sinitsa, R.J. Barber, R.N.

Tolchenov, J. Tennyson, J. Quant. Spectrosc. Radiat. Transfer 109, 1834-1844 (2008).

16. J.T. Hodges, D. Lisak, N. Lavrentieva, A. Bykov, L. Sinitsa, J. Tennyson, R.J. Barber, R.N. Tolchenov, J. Mol. Spectrosc. 249, 86-94 (2008).
17. A.D. Bykov, N.N. Lavrentieva, T.M. Petrova, L.N. Sinitsa, A.M. Solodov, R.J. Barber, J. Tennyson, R.N. Tolchenov, Optika i spectroscop. 105, 25-31 (2008).
18. N. Lavrentieva, A. Osipova, L. Sinitsa, Ch. Claveau, A. Valentin, Mol. Phys. 106, 1261-1266 (2008).
19. N.N. Lavrentieva, T.P. Mishina, L.N. Sinitsa, J. Tennyson, Atm. Oceanic Opt. 21, 1096-1100 (2008).
20. S.A. Tashkun, V.I. Perevalov, J.-L. Teffo, A.D. Bykov, N.N. Lavrentieva, CDSD-1000, J. Quant. Spectrosc. Radiat. Transfer 82, 165-196 (2003).
21. ftp://ftp.iao.ru/pub/CDSD-1000.
22. http://saga.atmos.iao.ru.
23. C.J. Tsao, B. Curnutte, J. Quant. Spectrosc. Radiat. Transfer 2, 41-91 (1962).
24. R.P. Leavitte, J. Chem. Phys. 73, 5432-5450 (1980).
25. A. Bykov, N. Lavrent'eva, and L. Sinitsa, Opt. Spektrosk. 83, 73-82 (1997).
26. A.D. Bykov, N.N. Lavrentieva, Atm. Opt. 4, 518-529 (1991).
27. K.M. Mack, J.S. Muenter, J. Chem. Phys. 66, 5278-5283 (1977).
28. A.Yu. Stepukhin, V.A. Udovenya, L.S. Kostyuchenko, Izv. Vyssh. Uch. Zaved. SSSR, Fizika, Dep. VINITI, No. 2182-B91 (1991).
29. C.H. Townes and A.L. Schawlow, Microwave spectroscopy, McGraw-Hill, New York, NY, 1955.
30. L.D. Landau and E.M. Lifshitz, Quantum Mechanics, Pergamon Press, New York, 1965.
31. P. Varanasi, J. Quant. Spectrosc. Radiat. Transfer 39, 13-25 (1988).

32. G. Wagner, M. Birk, R.R. Gamache, and J.M. Hartmann, J. Quant. Spectrosc. Radiat. Transfer 92, 211-230 (2005).

33. R.A. Toth, L.R. Brown, MA.H. Smith, V. M. Devi, D. C. Benner, M. Dulick, J. Quant. Spectrosc. Radiat. Transfer 101, 339-366 (2006).

34. R.R. Gamache and L.S. Rothman, Abstracts of the Xth Colloquium on High Resolution Molecular Spectroscopy, Dijon, 14-18 September 1987, p. 288.

35. H.M. Pickett, J. Chem. Phys. 73, 6090 (1980).

Table 1. Molecular and spectroscopic constants used in calculations.

	O_3	N_2	O_2
μ, D	-0.532	0	0
Q, D Å	Q_{xx} = -1.4	1.4	0.4
	Q_{yy} = -0.7		
	Q_{zz} = 2.1		
α, Å^3	α_i = 2.8	1.76	1.59
	α_i^{xx} =2.0		
	α_i^{yy} =1.8		
	α_i^{zz} = 4.6		
	α_f = 2.89 (101)		
	α_f^{zz} = 5.14 (101)		
	α_f = 2.85 (200)		
	α_f^{zz} = 5.01 (200)		
	α_f = 2.88 (002)		
	α_f^{zz} = 4.68 (002)		
I, 10^{-25}erg	2.126	2.485	2.003
B_0, cm^{-1}	-	1.998	1.4456
D_0, cm^{-1}	-	$5.76\cdot10^{-6}$	$4.839\cdot10^{-6}$

Table 2. Calculated and experimental [5] O_3-N_2(O_2) line shift coefficients δ (10^{-3} $cm^{-1}atm^{-1}$) and temperature exponents N for the $\nu_1+\nu_3$ band. **Lines used for fitting are marked with asterisk.**

J'	K_a'	K_c'	J	K_a	K_c	O_3-N_2			O_3-O_2	
						δ calc.	δ expt	N calc.	δ calc.	δ expt
42	2	41	43	2	42	-3.28	-4.2	0.78	-4.54	-5.3
38*	5	34	39	5	35	-3.25	-4.0	0.94	-4.69	-4.8
37	4	33	38	4	34	-2.60	-4.0	1.10	-3.73	-4.4
34	6	29	35	6	30	-3.37	-3.6	1.10	-4.71	-4.9
32	5	28	33	5	29	-2.92	-3.3	1.06	-4.22	-4.3
31	6	25	32	6	26	-3.27	-3.6	1.10	-4.53	-4.3
31	5	26	32	5	27	-2.80	-2.7	1.12	-3.99	-3.7
31	1	30	32	1	31	-2.85	-3.8	0.83	-4.06	-4.5
30	5	26	31	5	27	-2.86	-3.7	1.09	-4.15	-4.3
31	0	31	32	0	32	-3.52	-4.4	0.74	-4.76	-4.7
30	1	30	31	1	31	-3.50	-4.2	0.74	-4.76	-4.5
28	6	23	29	6	24	-3.14	-3.5	1.10	-4.37	-3.9
29	0	29	30	0	30	-3.48	-3.2	0.75	-4.72	-4.7
27	6	21	28	6	22	-3.11	-3.0	1.10	-4.33	-3.8
28	2	27	29	2	28	-2.89	-3.5	0.88	-4.12	-4.2
28	1	28	29	1	29	-3.46	-3.1	0.76	-4.71	-4.2
27	1	26	28	1	27	-2.66	-3.3	0.87	-3.82	-4.0
27*	0	27	28	0	28	-3.43	-3.3	0.75	-4.66	-3.8
25	5	20	26	5	21	-2.88	-3.0	1.15	-4.13	-3.4
25	3	22	26	3	23	-2.17	-2.9	1.08	-3.26	-3.5
24	6	19	25	6	20	-3.01	-3.0	1.10	-4.27	-3.3
25	1	24	26	1	25	-2.58	-3.1	0.90	-3.72	-4.0
24	5	20	25	5	21	-2.80	-3.0	1.13	-4.03	-3.5
24	4	21	25	4	22	-2.62	-3.2	1.05	-3.87	-4.0
23	6	17	24	6	18	-2.98	-2.4	1.11	-4.26	-3.5
22*	8	15	23	8	16	-3.24	-3.2	1.04	-4.68	-3.3
23	5	18	24	5	19	-2.78	-2.8	1.13	-4.01	-3.6
22	7	16	23	7	17	-3.14	-2.8	1.07	-4.52	-3.6
23	4	19	24	4	20	-2.38	-2.9	1.13	-3.53	-3.4
22	5	18	23	5	19	-2.73	-3.2	1.12	-3.95	-3.9
21	7	14	22	7	15	-3.10	-3.1	1.06	-4.49	-3.4
23	0	23	24	0	24	-3.27	-3.1	0.79	-4.56	-4.0
20	8	13	21	8	14	-3.14	-3.0	1.02	-4.45	-3.4
20	7	14	21	7	15	-3.06	-3.1	1.05	-4.41	-3.4
19	7	12	20	7	13	-3.02	-2.4	1.04	-3.37	-3.5
14	3	12	15	3	13	-2.25	-2.1	1.01	-3.45	-2.6
10	4	7	11	4	8	-2.28	-1.8	0.99	-3.39	-2.4
8	4	5	9	4	6	-2.25	-2.2	0.94	-3.36	-2.5
3*	2	1	2	2	0	-2.39	-2.0	0.81	-4.66	-1.2
27	0	27	26	0	26	-3.43	—	0.75	-4.53	-3.0
37	6	31	36	6	30	-3.26	—	1.09	-4.01	-3.3
37	2	35	36	2	34	-2.74	-3.2	1.03	-4.54	-3.9

Table 3. Statistics for $\Delta = \left| \delta^{expt} - \delta^{calc.} \right|$ values.

Δ, 10^{-3} $cm^{-1}atm^{-1}$	Percentage of lines	
	O_3-N_2	O_3-O_2
$\Delta \leq 1$	98%	87%
$1 < \Delta \leq 2$	2%	11%
$2 < \Delta \leq 3$	–	–
$3 < \Delta$	–	2%

Table 4. Calculated and experimental [6] O_3-N_2 line shift coefficients for the $2\nu_1$ band (10^{-3} $cm^{-1}atm^{-1}$). **Lines used for fitting are marked with asterisk.**

J'	K_a'	K_c'	J	K_a	K_c	calc.	expt
25*	6	20	26	7	19	-2.23	-1.9
28	5	23	29	6	24	-2.37	-1.7
14	7	7	15	8	8	-1.71	-1.8
28	4	24	29	5	25	-2.92	-1.5
24	4	20	25	5	21	-2.57	-1.7
29	3	27	30	4	26	-1.12	-1.2
13*	3	11	14	4	10	-2.11	-2.8
43*	1	43	44	0	44	-2.56	-2.5
42	0	42	43	1	43	-2.56	-3.4
18	2	16	19	3	17	-2.60	-2.4
32	0	32	33	1	33	-2.34	-2.2
37	4	34	38	3	35	-0.89	-1.7
25	1	25	26	0	26	-2.13	-1.2
25	2	24	26	1	25	-1.32	-2.7
17	1	17	18	0	18	-1.85	-2.1
12	0	12	13	1	13	-2.52	-1.7
15	2	14	16	1	15	0.04	-2.3

Table 5. Calculated and experimental [6] O_3-N_2 line shift coefficients for the $2\nu_3$ band (10^{-3} $cm^{-1}atm^{-1}$). **Lines used for fitting are marked with asterisk.**

J'	K_a'	K_c'	J	K_a	K_c	calc.	expt
8*	8	0	9	9	1	-3.95	-4.8
21*	8	14	21	9	13	-6.31	-7.0
26	6	20	26	7	19	-6.20	-6.2
18	6	12	18	7	11	-5.68	-5.2

Figure captions

Figure 1. Calculated and experimental [5] O_3-N_2 line shifting coefficients for the $\nu_1+\nu_3$ band. **The usual abscissa *J* is incremented by 0.1K_a in order to separate the transitions with identical *J* but different K_a values.**

Figure 2. Calculated and experimental [6] O_3-N_2 line shifting coefficients for the $2\nu_1$ band. **The usual abscissa *J* is incremented by 0.1K_a in order to separate the transitions with identical *J* but different K_a values.**

Figure 3. Calculated temperature dependence of the nitrogen-induced 25 5 20 ← 26 5 21 line shift in the $\nu_1+\nu_3$ band (upper panel) and the corresponding plot in logarithmic coordinates used to deduce the *N* value (lower panel).